Regulation of conductance by the number of fixed positive charges in the intracellular vestibule of the CFTR chloride channel pore

Jing-Jun Zhou, Man-Song Li, Jiansong Qi, and Paul Linsdell

Department of Physiology and Biophysics, Dalhousie University, Halifax, Nova Scotia B3H 1X5, Canada

Rapid chloride permeation through the cystic fibrosis transmembrane conductance regulator (CFTR) Cl^- channel is dependent on the presence of fixed positive charges in the permeation pathway. Here, we use site-directed mutagenesis and patch clamp recording to show that the functional role played by one such positive charge (K95) in the inner vestibule of the pore can be "transplanted" to a residue in a different transmembrane (TM) region (S1141). Thus, the mutant channel K95S/S1141K showed Cl^- conductance and open-channel blocker interactions similar to those of wild-type CFTR, thereby "rescuing" the effects of the charge-neutralizing K95S mutation. Furthermore, the function of K95C/S1141C, but not K95C or S1141C, was inhibited by the oxidizing agent copper(II)-*o*-phenanthroline, and this inhibition was reversed by the reducing agent dithiothreitol, suggesting disulfide bond formation between these two introduced cysteine side chains. These results suggest that the amino acid side chains of K95 (in TM1) and S1141 (in TM12) are functionally interchangeable and located closely together in the inner vestibule of the pore. This allowed us to investigate the functional effects of increasing the number of fixed positive charges in this vestibule from one (in wild type) to two (in the S1141K mutant). The S1141K mutant had similar Cl^- conductance as wild type, but increased susceptibility to channel block by cytoplasmic anions including adenosine triphosphate, pyrophosphate, 5-nitro-2-(3-phenylpropylamino)benzoic acid, and $Pt(NO_2)_4^{2-}$ in inside-out membrane patches. Furthermore, in cell-attached patch recordings, apparent voltage-dependent channel block by cytosolic anions was strengthened by the S1141K mutation. Thus, the Cl^- channel function of CFTR is maximal with a single fixed positive charge in this part of the inner vestibule of the pore, and increasing the number of such charges to two causes a net decrease in overall Cl^- transport through a combination of failure to increase Cl^- conductance and increased susceptibility to channel block by cytosolic substances.

The Journal of General Physiology

INTRODUCTION

Cystic fibrosis is caused by mutations in the CFTR, an epithelial cell Cl^- channel (Gadsby et al., 2006). A working model of the CFTR channel pore is emerging from a combination of imaging (Rosenberg et al., 2004; Mio et al., 2008), functional (Kidd et al., 2004; Linsdell, 2006), and molecular modeling (Mornon et al., 2008; Serohijos et al., 2008; Alexander et al., 2009) studies. Functionally, the pore is thought to have a relatively narrow region in which selectivity between anions is determined (Linsdell, 2006), flanked by intracellular and extracellular vestibules that use fixed positive charges to attract Cl^- ions to the pore (Smith et al., 2001; Linsdell, 2005; St. Aubin and Linsdell, 2006; Zhou et al., 2008). Functional evidence suggests that the inner vestibule of the pore is deeper and wider than the outer vestibule (Linsdell and Hanrahan, 1996a; Sheppard and Robinson, 1997; McCarty, 2000). Of the 12 transmembrane (TM) regions that make up the CFTR protein, current evidence suggests that TM6 plays a dominant role in determining functional interactions between the narrow pore region and permeating anions (Ge et al., 2004). TM1, TM5, and TM6 contribute to the inner vestibule (McDonough et al., 1994; Linsdell, 2005; St. Aubin and Linsdell, 2006), and TM6 and the extracellular loops between TM1 and TM2 and TM11 and TM12 contribute to the outer vestibule (Smith et al., 2001; Zhou et al., 2007, 2008; Fatehi and Linsdell, 2009).

Within the inner vestibule of the CFTR pore, different positively charged amino acid side chains have been shown to be involved in interactions with intracellular anions: K95 in TM1 (Linsdell, 2005), R303 in TM5 (St. Aubin and Linsdell, 2006), and possibly R352 in TM6 (St. Aubin and Linsdell, 2006; but see Cui et al., 2008). Each of these residues has been shown to play an electrostatic role in attracting Cl^- ions from the cytoplasmic solution into the pore, and this attractive effect

J.-J. Zhou and M.-S. Li contributed equally to this paper.
Correspondence to Paul Linsdell: paul.linsdell@dal.ca

J.-J. Zhou's present address is Dept. of Physiology, Fourth Military Medical University, Xi'an 710032, China.

M.-S. Li's present address is Dept. of Emergency and ICU of Norman Bethune Medical College at Jilin University, ChangChun 130021, China.

Abbreviations used in this paper: BHK, baby hamster kidney; CuPhe, copper(II)-*o*-phenanthroline; DTT, dithiothreitol; MTS, methanethiosulfonate; MTSES, (2-sulfonatoethyl) MTS; MTSET, [2-(trimethylammonium)ethyl] MTS; NPPB, 5-nitro-2-(3-phenylpropylamino)benzoic acid; PPi, pyrophosphate; TES, *N*-tris[hydroxymethyl]methyl-2-aminoethanesulfonate; TLCS, taurolithocholate-3-sulfate; TM, transmembrane.

The Rockefeller University Press $30.00
J. Gen. Physiol. Vol. 135 No. 3 229–245
www.jgp.org/cgi/doi/10.1085/jgp.200910327

has been found to be important in maximizing the overall rate of Cl^- permeation (Linsdell, 2005; St. Aubin and Linsdell, 2006). The positive charges associated with K95 and R303 also attract larger cytoplasmic anions to the pore, where they may act as open-channel blockers and interfere with Cl^- permeation (Linsdell, 2005; St. Aubin et al., 2007; Li and Sheppard, 2009). Effects of mutagenesis on interactions with different blockers provide some evidence that K95 and R303 may be located at different depths into the pore from their cytoplasmic end. Thus, relatively small blocker molecules interact with K95 in a voltage- and external $[Cl^-]$–dependent manner, whereas R303 interacts with larger blockers that produce voltage- and external $[Cl^-]$–independent block. This suggests that K95 is located more deeply into the pore from its cytoplasmic end, with R303 occupying a more superficial location (St. Aubin et al., 2007). Mutagenesis of all positively charged arginine and lysine residues in the TMs suggest that K95, R303, and R352 are the only fixed positive charges in the inner vestibule of the pore (St. Aubin and Linsdell, 2006). Collectively, these findings suggest that K95 plays a unique role in contributing a positive charge located relatively deeply within the pore from its cytoplasmic end.

Although the positive charge associated with K95 appears to play a crucial role in interactions with a range of small intracellular blockers (Linsdell, 2005), additional uncharged side chains within the TMs have also been suggested to influence the effects of such blockers, including S341 in TM6 and S1141 in TM12 (McDonough et al., 1994; Zhang et al., 2000). One possible explanation is that these residues are located close to K95 in the inner vestibule, allowing them to modify blocker interactions with this critical positive charge. Here, we use site-directed mutagenesis and functional analysis to explore the ability of fixed positive charges at different sites in the inner vestibule of the pore to support high Cl^- conductance and interactions with channel blockers. Our results show that the functional role played by the positive charge at K95 can be "transplanted" to TM12 by concurrent mutagenesis of K95 and S1141. We further suggest that one positive charge in this region of the inner vestibule of the pore is sufficient to maximize Cl^- conductance, and that the addition of a second charge is in fact detrimental to channel function, as it promotes open-channel block by cytoplasmic anions.

MATERIALS AND METHODS

Experiments were performed on baby hamster kidney (BHK) cells transiently transfected with different forms of human CFTR in the pIRES2-EGFP vector (Takara Bio Inc.), allowing coexpression of CFTR and green fluorescent protein. The CFTR backgrounds used were wild type (prepared as described in Gong et al., 2002a) or one in which all cysteines had been removed by mutagenesis ("cys-less" CFTR; prepared as described in Mense et al., 2006, and Li et al., 2009). Cys-less CFTR cDNA was provided by D. Gadsby (The Rockefeller University, New York, NY). Cys-less CFTR also included a mutation in the first nucleotide-binding domain (V510A) to increase protein expression in the cell membrane (Li et al., 2009). In both cases, DNA was transfected using Lipofectamine and Plus reagent (Life Technologies) as described in detail previously (Gong and Linsdell, 2003). Transiently transfected cells were maintained at 37°C (wild-type background) or 27°C (cys-less background) for 1–4 d before patch clamp experimentation, at which time they were identified by fluorescence microscopy. Mutations were introduced using the QuikChange site-directed mutagenesis system (Agilent Technologies) and verified by DNA sequencing.

In most cases, macroscopic and single-channel patch clamp recordings were made using the excised inside-out configuration of the patch clamp technique. In some cases (see Fig. 7 and Fig. S4), macroscopic currents were recorded from cell-attached patches on unstimulated cells expressing spontaneously active E1371Q-CFTR channels. For inside-out patch recording, CFTR channels were usually activated after patch excision and recording of background currents by exposure to 5–30 nM of PKA catalytic subunit plus MgATP (1 mM unless stated otherwise) in the cytoplasmic solution. Unless stated otherwise, macroscopic currents were recorded after treatment with 2 mM of sodium pyrophosphate (PPi) to maximize channel activity and ensure concurrence between macroscopic and unitary open-channel I-V relationships (Linsdell and Gong, 2002; Gong and Linsdell, 2003; Fatehi et al., 2007). To ensure maximal stimulation by PPi, this substance was added after the PKA- and ATP-activated current had reached a steady amplitude (for example, see Fig. 5). Because channels bearing the E1371Q mutation appeared to be spontaneously active even in the absence of ATP (see Fig. S4), inside-out patch recordings of this construct were made in the absence of PKA or ATP unless stated otherwise. Background current levels in these E1371Q mutants were determined at the end of the experiment by adding a high concentration (10 µM) of the specific CFTR inhibitor $CFTR_{inh}$-172 (Ma et al., 2002) to the cytoplasmic solution in excised inside-out membrane patches.

During inside-out patch recordings, intracellular (bath) solutions contained (in mM): 150 NaCl, 10 *N*-tris[hydroxymethyl]methyl-2-aminoethanesulfonate (TES), and 2 $MgCl_2$. In a small number of experiments, TES was replaced by 10 mM Tris. The extracellular (pipette) solution for both inside-out and cell-attached patches had either the same composition as the bath solution (high chloride solution) or 150 mM Na gluconate substituted for NaCl (low chloride solution). Intracellular channel blockers were added to the bath solution from stock solutions made up in normal bath solution, as described previously (Linsdell, 2005). The oxidizing agent copper(II)-*o*-phenanthroline (CuPhe) was prepared freshly before each experiment by mixing $CuSO_4$ (200 mM in distilled water) with 1,10 phenanthroline (200 mM in ethanol) in a 1:4 molar ratio, giving final added concentrations of 100 µM Cu^{2+} and 400 µM phenanthroline. Methanethiosulfonate (MTS) reagents (2-sulfonatoethyl) MTS (MTSES) and [2-(trimethylammonium)ethyl] MTS (MTSET) were initially prepared as 160-mM stock solutions and stored frozen at −20°C as small-volume aliquots until the time of use, when they were diluted in bath solution and used immediately. All solutions were adjusted to pH 7.4 using NaOH. All chemicals were obtained from Sigma-Aldrich, except PKA (Promega) and MTSES and MTSET (Toronto Research Chemicals).

Current traces were filtered at 50–100 Hz using an eight-pole Bessel filter, digitized at 250 Hz to 1 kHz, and analyzed using pCLAMP9 software (MDS Analytical Technologies). Single-channel current amplitudes were estimated from measurements of the mean amplitudes of at least 20 individual open-closed transitions

and, where possible, verified from all-point amplitude histograms constructed from periods of channel activity lasting 30–210 s. Macroscopic I-V relationships were constructed using depolarizing voltage ramp protocols, with a rate of change of voltage of 100 mV s^{-1} (Linsdell and Hanrahan, 1996a, 1998), or from 400-ms duration voltage steps from a holding potential of 0 mV (when using high extracellular Cl^- concentrations) or +60 mV (for low extracellular Cl^- concentrations). In both cases, background (leak) currents recorded before the addition of PKA and ATP have been subtracted digitally, leaving uncontaminated CFTR currents (Linsdell and Hanrahan, 1998; Gong and Linsdell, 2003). For E1371Q mutant channels, background currents were determined after the addition of 10 μM $CFTR_{inh}$-172 (see above). Membrane voltages were corrected for liquid junction potentials calculated using pCLAMP9 software. Where on-cell recordings are used (Fig. 7), membrane potential is given as applied pipette potential (V_p) due to uncertainty concerning the cell resting membrane potential.

As in previous studies of open-channel blockers (Linsdell and Hanrahan, 1999; Gong et al., 2002b; Zhou et al., 2007), the effects of 5-nitro-2-(3-phenylpropylamino)benzoic acid (NPPB), taurolithocholate-3-sulfate (TLCS), lonidamine, and $Pt(NO_2)_4^{2-}$ on macroscopic current amplitude were analyzed using the simplest version of the Woodhull (1973) model of voltage-dependent block:

$$I / I_0 = K_d(V) / \left(K_d(V) + [B]\right), \quad (1)$$

where I is the current amplitude in the presence of blocker, I_0 is the control, unblocked current amplitude, [B] is the blocker concentration, and $K_d(V)$ is the voltage-dependent apparent dissociation constant, the voltage dependence of which is given by:

$$K_d(V) = K_d(0)\ \exp(-z\delta VF / RT), \quad (2)$$

where zδ is the effective valence of the blocking ion (actual valence z multiplied by the fraction of the TM electric field apparently experienced during the blocking reaction), and F, R, and T have their usual thermodynamic meanings.

The effects of ATP concentration on macroscopic current amplitude were estimated using voltage steps lasting 400 ms. Because of the effects of ATP on CFTR channel gating, these experiments were performed in an E1371Q background. To maintain a constant Mg^{2+} concentration, Na_2ATP was added to the bath from concentrated stock solutions to give the desired total intracellular concentration of ATP. Mean current was averaged over the last 50 ms of the voltage step and compared with current in the absence of ATP to calculate the fractional unblocked current. This was then used to estimate the K_d for ATP inhibition according to the equation:

$$\text{Fractional unblocked current} = 1 / \left(1 + \left([ATP] / K_d\right)^{nH}\right), \quad (3)$$

where n_H is a slope factor of the concentration–inhibition relationship, or Hill coefficient. Analysis of ATP concentration-dependent effects by this method assumes that ATP is a single species. In fact, ATP exists as several different charged species, the concentrations of which were calculated using a computer program that corrects association constants for temperature and pH (Brooks and Storey, 1992). Major ATP species at each total ATP concentration used are given in Table I.

Experiments were performed at room temperature (21–24°C). Values are presented as mean ± SEM. Tests of significance were performed using a Student's two-tailed t test unless stated otherwise.

Online supplemental material

The online supplemental material includes seven figures. Fig. S1 shows the inhibitory effects of TLCS and lonidamine on wild type, K95S, K95S/S341K, and K95S/S1141K-CFTR. Fig. S2 shows single-channel recordings of K95S/S341K and S341K. Fig. S3 shows the apparent time- and voltage-dependent inhibition of S1141K by intracellular ATP in inside-out patches. Fig. S4 compares the activity of wild type and E1371Q in on-cell and inside-out membrane patches. Fig. S5 shows the block of wild type, S1141K, and S341K by intracellular NPPB. Fig. S6 shows the block of E1371Q and E1371Q/S1141K by intracellular $Pt(NO_2)_4^{2-}$ ions. Fig. S7 shows the predicted locations of K95, S341, and S1141 in two different published homology models of the CFTR pore region. Figs. S1–S7 are available at http://www.jgp.org/cgi/content/full/jgp.200910327/DC1.

RESULTS

An important pore-lining positive charge can be "moved" from TM1 to TM12

Lysine K95 in TM1 plays a key role in the attraction of small intracellular open-channel blockers to the CFTR pore (Linsdell, 2005). One example of a blocker that interacts with the positive charge at this site is NPPB (Linsdell, 2005). As shown in Fig. 1, the addition of 50 μM NPPB to the intracellular solution caused a potent, voltage-dependent inhibition of macroscopic currents carried by wild-type CFTR in inside-out membrane patches with a low extracellular Cl^- concentration. Consistent with previous findings with other K95 mutants (Linsdell, 2005), removal of the positive charge at K95 in the K95S mutation is associated with significant reduction in the apparent potency of block by NPPB (Fig. 1, A and B). Woodhull analysis suggests that the apparent K_d (at 0 mV) is increased approximately sevenfold, from 12.4 ± 1.7 μM (n = 4) in wild type to 90.4 ± 17.6 μM (n = 4) in K95S (Fig. 1, B and D), without a significant change in apparent blocker voltage dependence (apparent valence, zδ, of −0.20 ± 0.02 [n = 4] in wild type and −0.16 ± 0.02 [n = 4] in K95S; $P > 0.2$).

In a K95S background, the introduction of a positive charge in either TM6 (S341K) or TM12 (S1141K) led to a significant increase in the apparent potency of NPPB block compared with K95S alone (Fig. 1), with mean $K_d(0)$ values of 35.8 ± 2.0 μM (n = 4) in K95S/S341K and 10.5 ± 1.8 μM (n = 4) in K95S/S1141K (Fig. 1 D), again with no significant change in apparent voltage dependence of block (zδ of −0.17 ± 0.02 [n = 4] in K95S/S341K and −0.22 ± 0.03 [n = 4] in K95S/S1141K). In fact, in the K95S/S1141K mutant, the apparent K_d was not significantly different than that observed in wild type ($P > 0.4$; Fig. 1 D), suggesting that the role played by the positive charge at position 95 in the interaction between NPPB and the pore can be completely recovered by moving this positive charge from TM1 to TM12. Similar results were obtained with two other blockers that show strong interactions with K95, TLCS, and lonidamine (Fig. S1).

TABLE I

Major ATP species at each ATP concentration used

Overall [ATP]	$[Mg_2ATP^0]$	$[MgATP^{2-}]$	$[HATP^{3-}]$	$[NaATP^{3-}]$	$[ATP^{4-}]$
0.3	0.013 (4.2%)	0.25 (84.8%)	0.002 (0.8%)	0.021 (7.0%)	0.009 (3.0%)
1.0	0.027 (2.7%)	0.81 (81.4%)	0.011 (1.1%)	0.10 (10.2%)	0.044 (4.4%)
3.0	0.014 (0.5%)	1.68 (56.1%)	0.094 (3.1%)	0.84 (28.0%)	0.37 (12.2%)
10.0	0.003 (0.0%)	1.93 (19.3%)	0.56 (5.6%)	5.20 (52.0%)	2.30 (23.0%)

For each overall ATP concentration given (in mM), the concentration (mM) and percentage of total ATP were calculated as described in Materials and methods.

The positive charge at K95 is also important for attracting Cl^- ions into the pore, and removal of this charge by mutagenesis is associated with a dramatic decrease in unitary Cl^- conductance (Ge et al., 2004). This effect is clear in the K95S mutant, where unitary Cl^- currents appear close to the resolution for single-channel recording (Fig. 2 A). Although difficult to resolve unequivocally, the conductance of K95S channels appears to be <20% of wild-type conductance (Fig. 2, A and C), which was 8.27 ± 0.06 pS (n = 9) at hyperpolarized voltages and 7.94 ± 0.02 pS (n = 5) at depolarized voltages (Fig. 2 E). As with the open-channel blocker experiments described above, the introduction of a positive charge in TM12 led to a significant recovery of wild-type pore properties—in this case, a dramatic increase in unitary conductance in the K95S/S1141K double mutant compared with K95S alone (Fig. 2). In the K95S background, the second site mutation (S1141K)

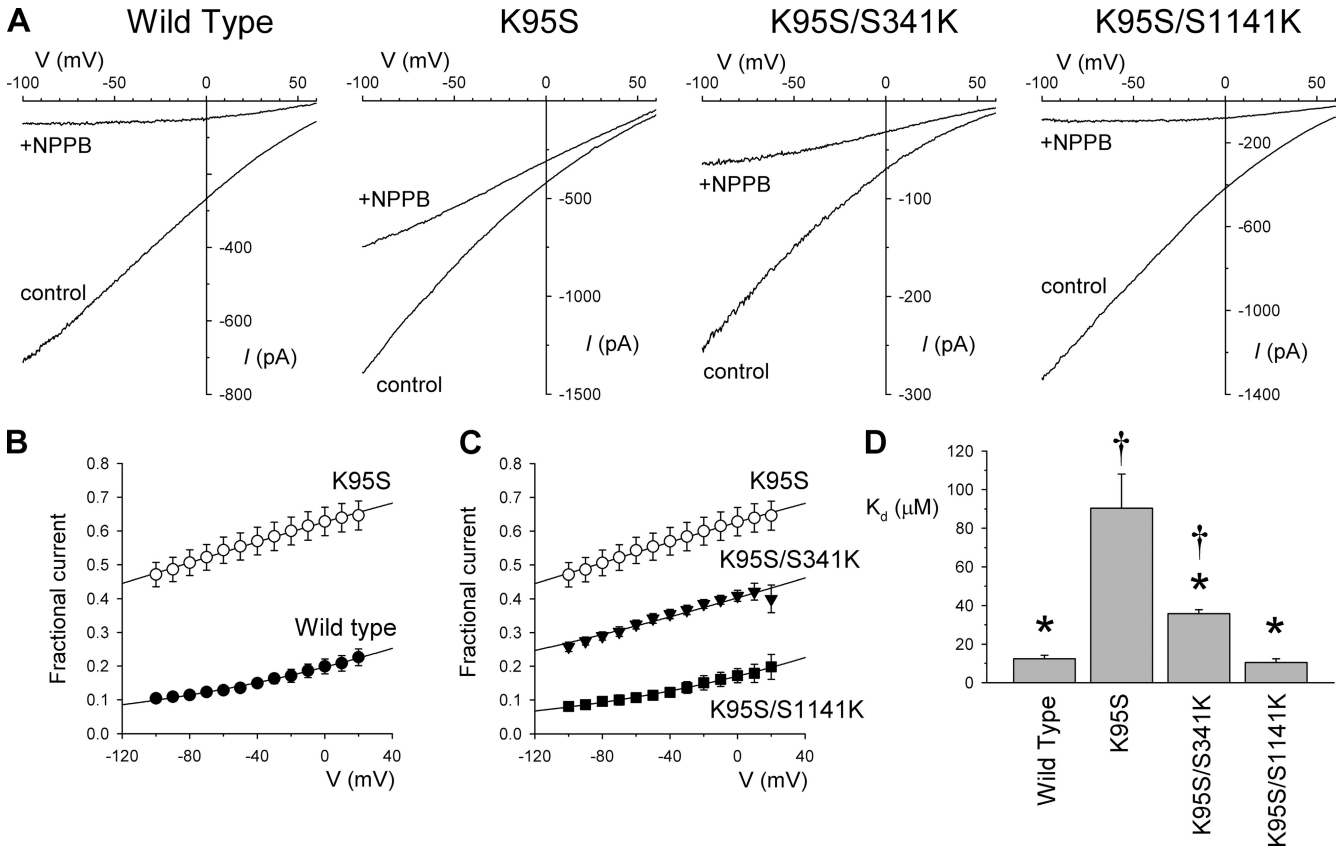

Figure 1. Block by NPPB depends on the presence of a positive charge in the pore. (A) Example leak-subtracted macroscopic I-V relationships for the different CFTR variants named using a low extracellular Cl^- concentration (4 mM) after maximal channel activation with 5–10 nM PKA, 1 mM ATP, and 2 mM PPi. In each case, currents were recorded before (control) and after the addition of 50 μM NPPB to the intracellular (bath) solution. (B and C) Mean fractional current remaining after the addition of NPPB as a function of voltage. ●, wild type (B); ○, K95S (B and C); ▼, K95S/S341K (C); ■, K95S/S1141K (C). Each set of data has been fit by Eq. 1, giving for wild-type: $K_d(0)$ = 12.3 ± 0.1 μM and $z\delta$ = −0.20 ± 0.01; for K95S: $K_d(0)$ = 83.9 ± 0.6 μM and $z\delta$ = −0.16 ± 0.00; for K95S/S341K: $K_d(0)$ = 33.7 ± 0.7 μM and $z\delta$ = −0.15 ± 0.01; and for K95S/S1141K: $K_d(0)$ = 10.3 ± 0.1 μM and $z\delta$ = −0.22 ± 0.01. (D) Mean $K_d(0)$ values obtained from similar analysis of data from individual patches. Asterisks indicate a significant difference from K95S, and daggers indicate a significant difference from wild type ($P < 0.05$ in both cases). Mean of data from four patches in B–D.

restored conductance at hyperpolarized voltages to 6.28 ± 0.06 pS (n = 9), ~75% of wild-type values, and at depolarized voltages to 5.37 ± 0.04 pS (n = 10), ~67% of wild type (Fig. 2 E). Interestingly, the S1141K mutation alone led to a small but significant reduction in unitary conductance compared with wild type, to 8.02 ± 0.08 pS

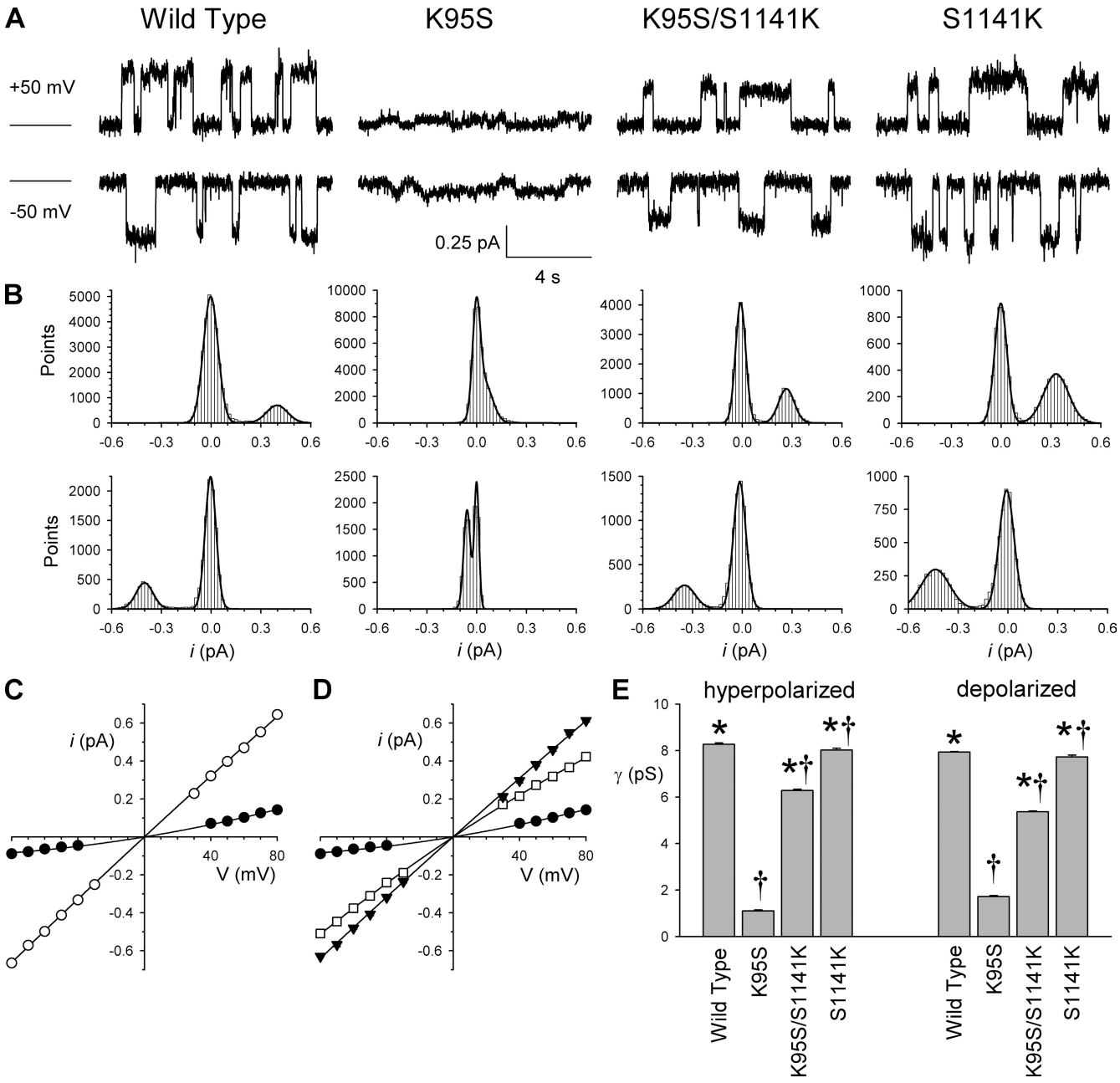

Figure 2. Single-channel conductance is restored by moving a positive charge from TM1 to TM12. (A) Example single-channel currents carried by the different CFTR variants named, using symmetrical high (154-mM) Cl^- concentrations, at membrane potentials of +50 mV (top) and −50 mV (bottom). Channel activity was maintained by the addition of 15–30 nM PKA and 1 mM ATP to the bath. The line to the left represents the closed-channel current level. (B) All-points amplitude histograms prepared from extended periods of the recordings shown in A. Each has been fitted by the sum of two Gaussian functions with mean amplitudes of 0 pA and at +50 mV: 0.397 pA (wild type), 0.046 pA (K95S), 0.266 pA (K95S/S1141K), and 0.331 pA (S1141K); at −50 mV: −0.401 pA (wild type), −0.058 pA (K95S), −0.349 pA (K95S/S1141K), and −0.437 pA (S1141K). After fitting, the width of the bins has been increased from 0.005–0.01 to 0.02 pA for display purposes. (C and D) Mean single-channel I-V relationships for wild-type (C, ○), K95S (C and D, ●), K95S/S1141K (D, □), and S1141K (D, ▼). (E) Mean unitary slope conductance measured from individual patches for inward currents (hyperpolarized voltages) and outward currents (depolarized voltages). Asterisks indicate a significant difference from K95S ($P < 10^{-10}$). Daggers indicate a significant difference from wild type ($P < 10^{-10}$ for both K95S and K95S/S1141K; $P < 0.05$ for S1141K). Mean of data from 4–10 patches in C–E.

($n = 4$) at hyperpolarized voltages and to 7.72 ± 0.08 pS ($n = 5$) at depolarized voltages (Fig. 2 E).

In contrast to these results with S1141, S341 mutants were not able to support high Cl^- conductance (Fig. S2). Thus, the S341K mutant was associated with very small unitary currents that were difficult to resolve unequivocally when introduced into either a wild-type or a K95S background (Fig. S2). Although difficult to quantify accurately, these unitary currents had apparent amplitudes <20% of wild type.

Physical proximity of K95 and S1141

The results described above suggest that the important positive charge at K95 in TM1 can be transplanted to residue 1141 in TM12, and that these two residues are functionally interchangeable. One possible explanation for this interchangeability might be that the pore-lining side chains of these two residues may be located physically close together within the inner vestibule. We tested this hypothesis by attempting to chemically cross-link cysteine residues substituted for these two

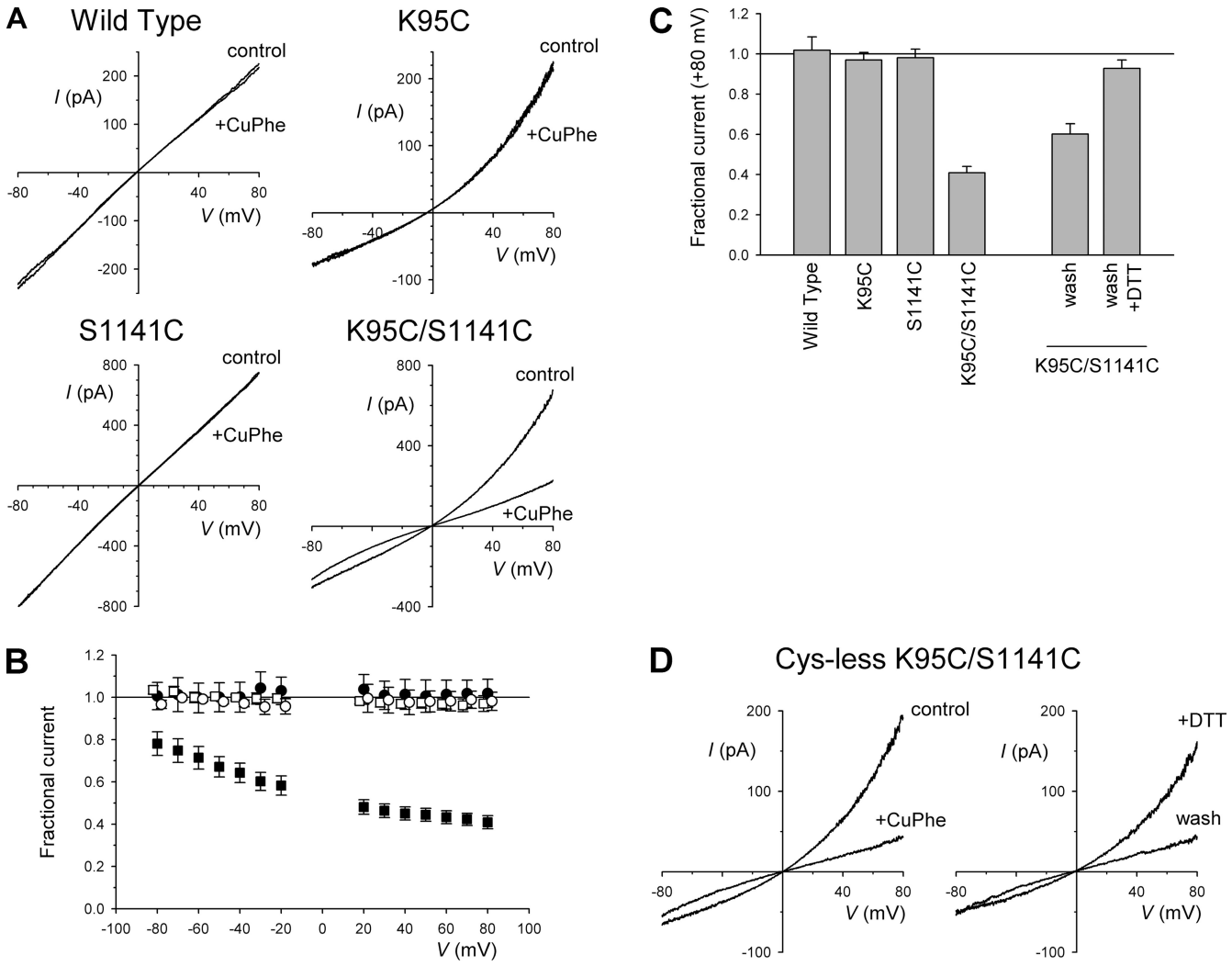

Figure 3. Cross-linking of cysteines substituted for K95 and S1141. (A) Example leak-subtracted macroscopic I-V relationships for the different CFTR variants named, using symmetrical high (154-mM) Cl^- concentrations, after maximal channel activation with 5–10 nM PKA, 1 mM ATP, and 2 mM PPi. Currents were recorded before (control) and after the addition of CuPhe to the intracellular (bath) solution. (B) Mean fractional current remaining after the addition of CuPhe as a function of voltage in wild type (●), K95C (□), S1141C (○), and K95C/S1141C (■). Data values for K95C/S1141C were significantly different from wild type, K95C, or S1141C ($P < 0.05$ in each case) at all voltages examined. (C) Mean fractional current remaining after the addition of CuPhe at +80 mV for different channel variants as indicated, and for K95C/S1141C after washing with normal bath solution (wash) or with bath solution supplemented with 5 mM DTT (wash + DTT). Mean of data from three to nine patches in B and C. (D) Example leak-subtracted macroscopic I-V relationships for cys-less K95C/S1141C-CFTR recorded under the same conditions as in A. Both panels are from the same inside-out membrane patch before (control) and after the addition of 400 µM CuPhe to the intracellular (bath) solution (left), and after the removal of CuPhe and reapplication of ATP, PKA, and PPi (wash) and subsequent application of 5 mM DTT (right, +DTT). Representative example of five patches.

residues. The K95C/S1141C double mutant generated small macroscopic currents that showed outward rectification under symmetrical Cl^- concentration conditions (Fig. 3), as observed with all mutations that remove the charge at K95 (Linsdell, 2005), including K95C (Fig. 3). K95C/S1141C currents in inside-out patches were insensitive to the application of 5 mM of the reducing agent dithiothreitol (DTT; not depicted), suggesting that spontaneous disulfide bond formation between the two cysteine side chains is either negligible or without functional consequence. However, the oxidizing reagent CuPhe, which has been used to induce disulfide bond formation between introduced cysteines in other parts of the CFTR protein (Mense et al., 2006; Loo et al., 2008; Serohijos et al., 2008), led to a strong reduction in current amplitude in K95C/S1141C (Fig. 3, A–C), suggesting a functional modification of the protein. This inhibition was apparently stronger at depolarized than at hyperpolarized potentials (Fig. 3 B), with the result that current rectification was greatly reduced after CuPhe treatment. Interestingly, neither wild-type CFTR currents nor the single mutants K95C or S1141C appeared sensitive to CuPhe under these conditions (Fig. 3, A–C), consistent with this agent acting by causing cross-linking of the two cysteine side chains introduced at these positions. Inhibition of K95C/S1141C by CuPhe was only partially reversed by washing; however, the degree of reversibility was significantly enhanced by the inclusion of 5 mM DTT in the wash solution (Fig. 3 C), consistent with CuPhe inhibition reflecting some oxidative process. Overall, washing restored 26.7 ± 3.5% of CuPhe-sensitive current at +80 mV ($n = 3$), whereas washing plus DTT restored 85.5 ± 3.5% of CuPhe-sensitive current at this voltage ($n = 4$; $P < 0.01$ vs. wash alone). A K95C/S341C double mutant did not yield functional currents in inside-out patches either without or after treatment with 5 mM DTT.

Although these results suggest that K95C can be cross-linked to S1141C, they are potentially confounded by the presence of endogenous cysteine side chains in the CFTR protein. We therefore introduced these two mutations into a functional cys-less version of CFTR (Mense et al., 2006; Li et al., 2009; see Materials and methods). As shown in Fig. 3 D, cys-less K95C/S1141C also generated small, outwardly rectified currents in inside-out membrane patches that showed the same apparent sensitivity to CuPhe as that described above for these mutations in a wild-type background. On average, the application of CuPhe reduced current amplitude in cys-less K95C/S1141C by 84.7 ± 5.2% at +80 mV ($n = 5$). Washing CuPhe from the bath restored only 6.7 ± 3.7% of CuPhe-sensitive current at this voltage ($n = 5$), whereas subsequent exposure to 5 mM DTT restored 76.8 + 3.5% of CuPhe-sensitive current ($n = 5$). K95C/S1141C channel currents were also potently inhibited by the addition of 100 µM Cu^{2+} alone to the bath; however, these effects were fully reversed simply by washing the Cu^{2+} ions from the bath (not depicted). In an interesting contrast to these effects, K95C/S1141C currents were not significantly affected by the addition of 300 µM Cd^{2+} ions (not depicted).

The use of cys-less CFTR also allowed us to confirm that the side chains of K95, S341, and S1141 are exposed within the inner vestibule of the CFTR channel pore using cysteine-reactive reagents. This was not possible previously because commonly used cysteine-reactive reagents, MTSES and MTSET, potently inhibit the activity of wild-type CFTR when applied to the cytoplasmic face of the membrane (St. Aubin and Linsdell, 2006). However, we have recently shown that cys-less CFTR is not subject to irreversible modification by these reagents, although high concentrations of MTSES apparently lead to reversible inhibition by open-channel block (Li et al., 2009). As shown in Fig. 4, the application of 200 µM of negatively charged MTSES or 2 mM of positively charged MTSET to the intracellular solution had no effect on macroscopic current amplitude in cys-less CFTR. In contrast, each of the mutants, K95C, S341C, and S1141C (all in a cys-less background), was strongly sensitive to both MTSES and MTSET. In each case, currents were strongly inhibited by MTSES, consistent with an inhibitory effect of depositing a large, negatively charged reagent in the permeation pathway. In contrast, MTSET inhibited currents carried by cys-less S341C and cys-less S1141C, but potentiated currents carried by cys-less K95C. In S341C and S1141C, modification by the bulky MTSET molecule may partly occlude the pore, reducing Cl^- current. In contrast, in K95C, deposition of positive charge by reaction with MTSET may replace the function of the positive charge at this site that is lost as a consequence of the K95C mutation. Consistent with this idea, MTSET modification converts the cys-less K95C I-V relationship from outwardly rectified (before modification) to linear or mildly inwardly rectified after modification (Fig. 4 B). Thus, the functional effects of MTSET were significantly greater at hyperpolarized than at depolarized voltages (Fig. 4 C), and the shape of the I-V relationship was quantitatively different after modification, with the current amplitude at −80 mV relative to that at +80 mV being increased from 0.33 ± 0.04 ($n = 10$) before modification to 1.33 ± 0.10 ($n = 10$) after MTSET treatment ($P < 0.001$, paired t test). In all cases, the effects of MTS reagents were not reversed by washing these reagents from the bath, but could be reversed by the application of 2–5 mM DTT. The strong reactivity of cys-less K95C, S341C, and S1141C to intracellular MTSES and MTSET is consistent with the cysteine side chains introduced at these positions being exposed within the aqueous inner vestibule of the pore.

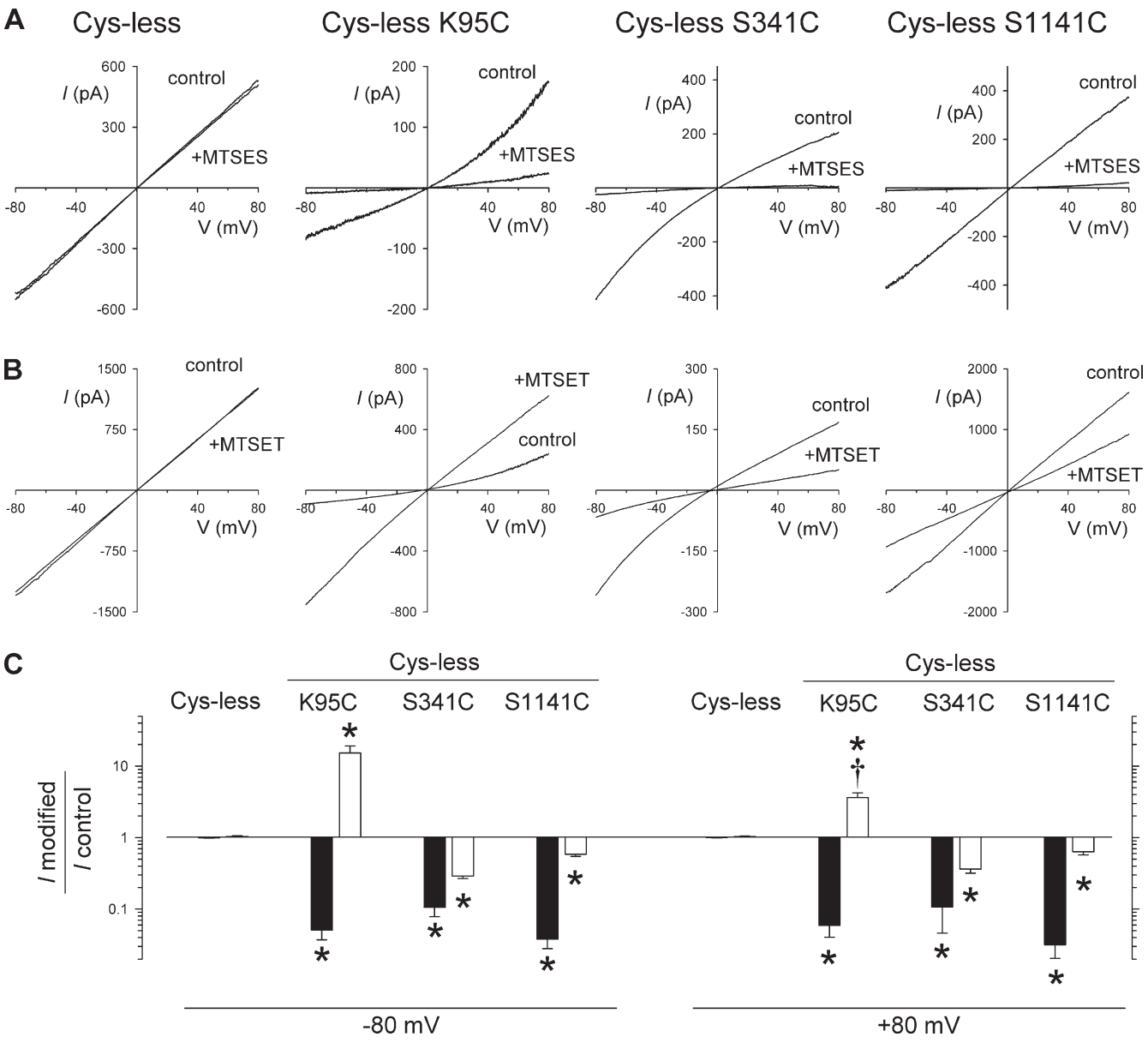

Figure 4. Modification of cysteines in the inner vestibule of the pore by intracellular MTS reagents. (A and B) Example leak-subtracted macroscopic I-V relationships for different CFTR variants (in a cys-less background), using symmetrical high (154-mM) Cl^- concentrations, after maximal channel activation with 5–10 nM PKA, 1 mM ATP, and 2 mM PPi. Currents were recorded before (control) and after the addition of 200 µM MTSES (A) or 2 mM MTSET (B) to the intracellular (bath) solution. (C) Mean effect of MTSES (filled bars) or MTSET (open bars) on macroscopic current amplitude at −80 mV (left) and +80 mV (right). Asterisks indicate a significant difference from cys-less ($P < 0.05$). Daggers indicate a significant difference from the same treatment at −80 mV ($P < 0.05$, paired *t* test). Mean of data from 3–10 patches.

Adding an extra positive charge to the inner vestibule of the pore results in channel block

The results described above suggest that K95 in TM1 and S1141 in TM12 are both functionally interchangeable and physically close together in the inner vestibule of the pore. We were therefore interested to know how the presence of two adjacent positive charges in this region of the inner vestibule—as presumably exist in the S1141K single mutant—would influence interactions with open-channel blockers. However, when we investigated the S1141K mutant at the macroscopic current level using depolarizing voltage ramp protocols like those used in Fig. 1, it became apparent that channel function had been altered in a way we had not anticipated from our initial single-channel experiments (see Fig. 2). With a low extracellular Cl^- concentration, macroscopic currents in S1141K showed outward rectification leading to a flattening of the I-V relationship at hyperpolarized voltages (Fig. 5, A and B). Furthermore, when 2 mM PPi was applied to maximize channel activity,

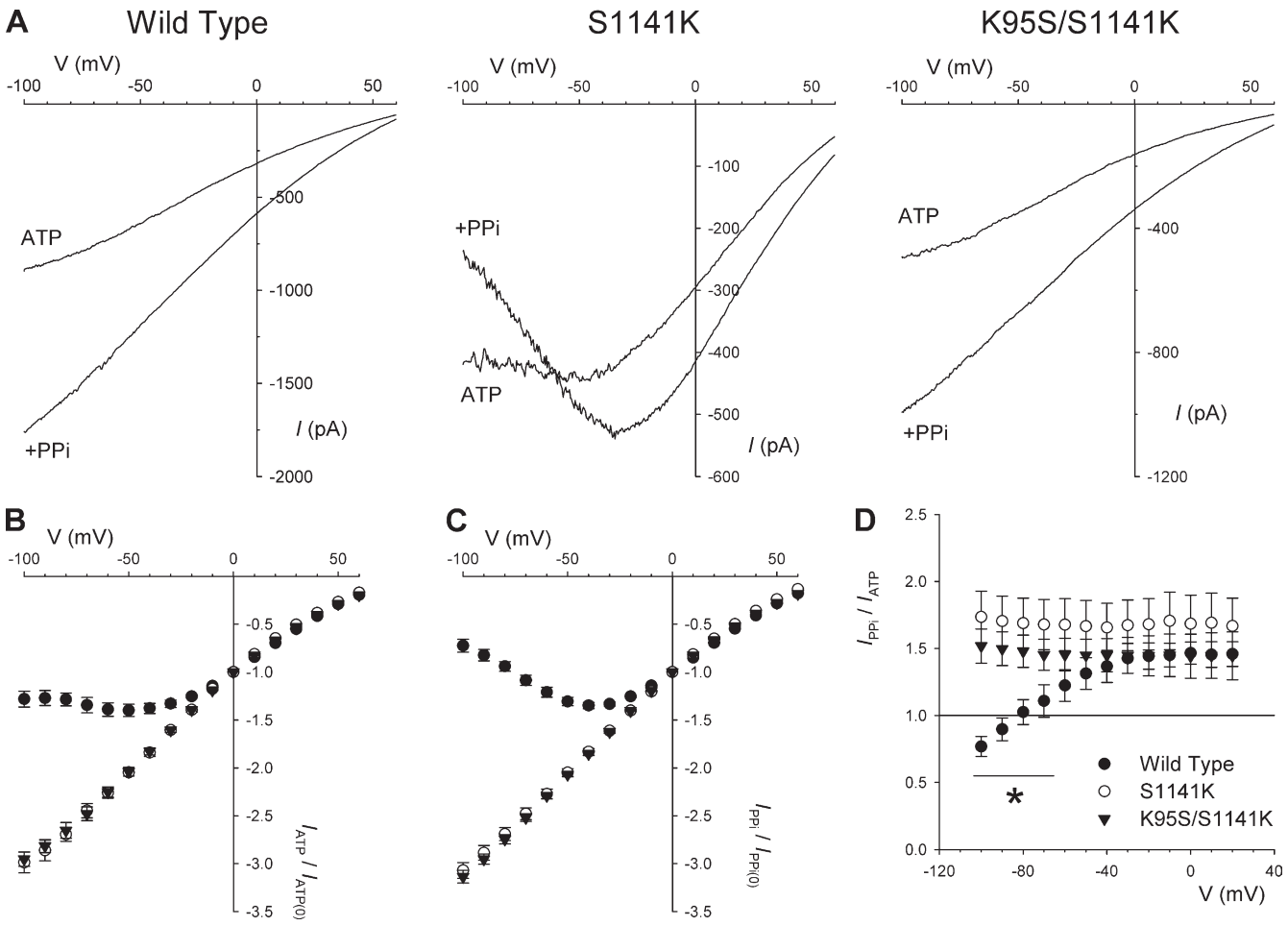

Figure 5. Apparent inhibition of S1141K at hyperpolarized voltages. (A) Example leak-subtracted macroscopic I-V relationships for the different CFTR variants named using a low extracellular Cl^- concentration (4 mM). In each case, currents were recorded after stimulation with 5–10 nM PKA and 1 mM ATP (ATP), and again after the addition of 2 mM PPi (+PPi). (B and C) Relative shape of the I-V relationship in the presence of 1 mM ATP (B) or 1 mM ATP plus 2 mM PPi (C), analyzed by plotting the current at each voltage relative to the current amplitude at 0 mV, for wild type (○), S1141K (●), and K95S/S1141K (▼). (D) The effect of PPi on macroscopic current amplitude. Note that PPi causes a voltage-independent stimulation in wild type (○) and K95S/S1141K (▼), whereas in S1141K (●), PPi causes stimulation at depolarized voltages and inhibition at hyperpolarized voltages. Asterisk indicates the voltage range over which the effects of PPi on wild type and S1141K were significantly different ($P < 0.05$). Mean of data from four to five patches in B–D.

rectification became even more pronounced, leading to a region of negative slope conductance below ~−30 mV (Fig. 5, A and C). As a result, although PPi stimulated macroscopic current amplitude in S1141K at depolarized voltages, it actually inhibited current at the most hyperpolarized voltages studied (Fig. 5 D). None of these effects was observed in wild type or K95S/S1141K, two channel variants with a single positive charge in this part of the inner vestibule of the pore (Fig. 5), or in S341K (not depicted).

Because the S1141K mutant did not strongly affect either unitary conductance or the linearity of the I-V relationship under symmetrical high Cl^- conditions (Fig. 2), we considered that the unusual I-V shape shown in Fig. 5 might reflect voltage-dependent block of S1141K by some negatively charged substance present in our intracellular solutions. However, the solutions used in the experiments shown in Fig. 5 were very simple ones, containing only NaCl, $MgCl_2$, TES buffer, MgATP, and PKA (see Materials and methods). Replacing the anionic TES buffer with the cationic pH buffer Tris did not alter the unusual shape of the I-V relationship in S1141K (not depicted). In contrast, altering the ATP concentration did lead to striking time- and voltage-dependent changes in current amplitude that suggest an inhibitory effect of ATP on S1141K (Fig. S3).

Analysis of the apparent inhibitory effect of ATP is complicated by the complex effects of ATP on CFTR channel gating (Hwang and Sheppard, 2009; Muallem and Vergani, 2009). One way to avoid this complication would be to use a CFTR variant in which ATP-dependent gating was abolished. Mutation of a key Walker B glutamate residue in the second nucleotide-binding domain, E1371, prevents ATP hydrolysis and leads to a dramatic

prolongation of CFTR channel open times (Vergani et al., 2003; Gadsby et al., 2006; Stratford et al., 2007). To our surprise, we found that the E1371Q mutant was constitutively active in on-cell recordings from intact BHK cells, and that even after excision into nominally ATP-free solutions, channel activity remained maximal (Fig. S4). Although the reasons for this constitutive activity, which contrasts with a complete lack of spontaneous activity we observe for other CFTR constructs expressed in BHK cells, are unknown, it did allow us to quantify ATP effects on S1141K current amplitude in an E1371Q background in inside-out membrane patches, beginning with 0 ATP control conditions (Fig. 6). With a low extracellular Cl^- concentration (4 mM), the addition of 10 mM ATP caused a potent inhibition of S1141K/E1371Q current during 400-ms hyperpolarizing voltage steps from a holding potential of +60 mV (Fig. 6 A). Time-dependent inhibition by ATP was still apparent; however, use of the E1371Q background provides direct evidence that ATP inhibits current flow because the amplitude of the current is greatly reduced. Concentration-dependent effects of ATP under these experimental conditions, quantified from the amplitudes of macroscopic currents measured over the last 50 ms of the 400-ms voltage step, are shown in Fig. 6 B. The fitting of these results by Eq. 3 suggests a K_d of 1.92 mM at −100 mV. In contrast to the strong inhibition of S1141K/E1371Q current by ATP under these conditions, 10 mM

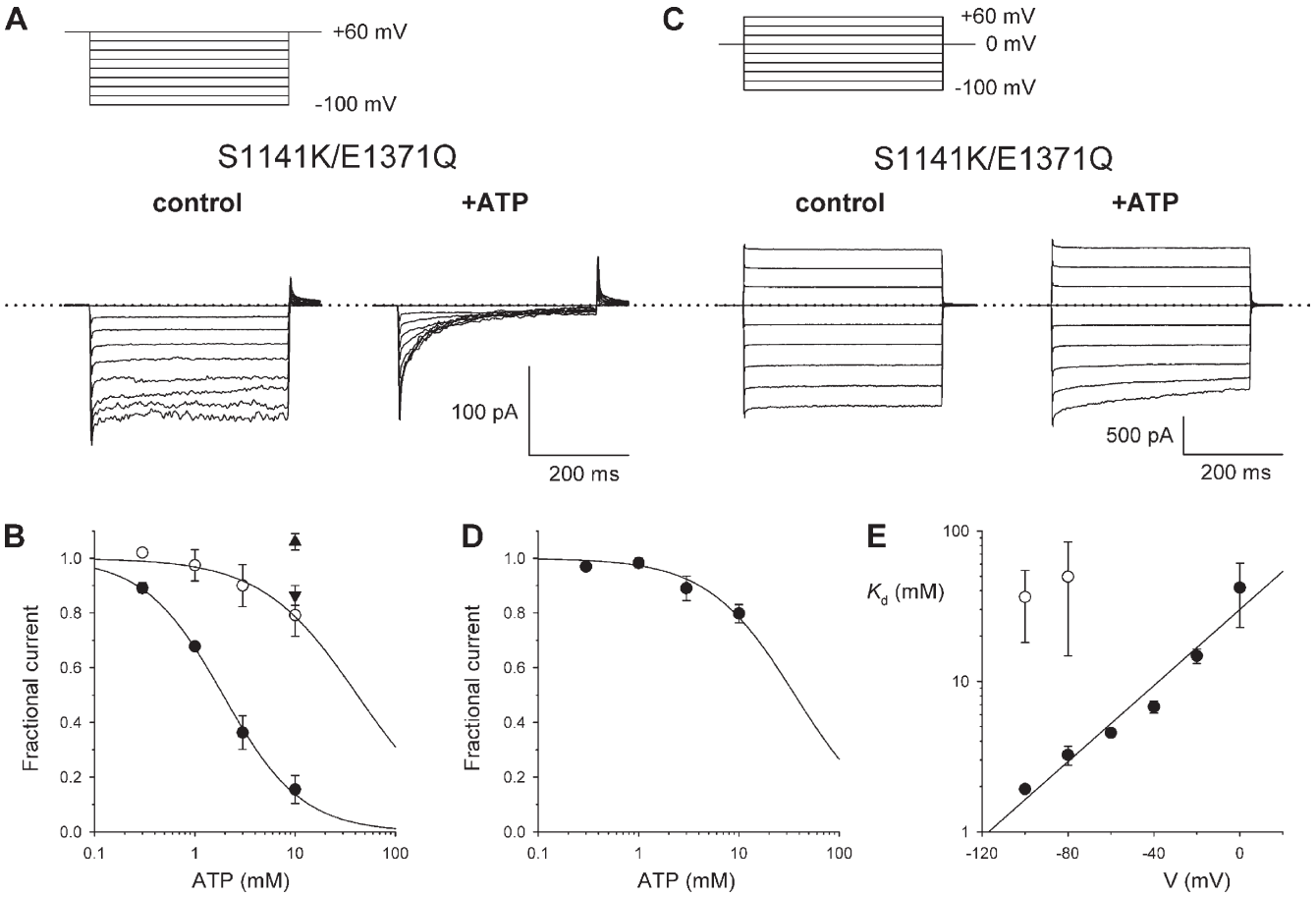

Figure 6. Inhibition of S1141K/E1371Q-CFTR by intracellular ATP. (A) Example macroscopic currents carried by S1141K/E1371Q during hyperpolarizing voltage steps to between +60 and −100 mV recorded under conditions of low extracellular Cl^- concentration (4 mM). Currents were recorded before (control) and immediately after the addition of 10 mM Na_2ATP to the intracellular solution in the absence of PKA and PPi. (B) Mean fractional current remaining after the addition of different concentrations of ATP under these conditions, measured at membrane potentials of −100 mV (●) and 0 mV (○). Fits are to Eq. 3, giving K_d = 1.92 ± 0.08 mM and n_H = 1.11 ± 0.05 at −100 mV, and K_d = 41.9 ± 19.1 mM and n_H = 0.91 ± 0.23 at 0 mV. Also shown are the effects of 10 mM ATP on E1371Q (▲) and K95S/S1141K/E1371Q (▼) at −100 mV. (C) Example macroscopic S1141K/E1371Q currents during voltage steps to between +60 and −100 mV recorded with a high extracellular Cl^- concentration (154 mM) before (control) and after the addition of 10 mM Na_2ATP to the intracellular solution in the absence of PKA. (D) Mean fractional current remaining after the addition of different concentrations of ATP under these conditions, measured at a membrane potential of −100 mV. The data are fit to Eq. 3, giving K_d = 36.3 ± 18.2 mM when n_H was constrained to unity. (E) Voltage dependence of K_d estimated from fits such as those shown in B and D, with 4 mM Cl^- (●) and 154 mM Cl^- (○) in the extracellular solution. Data at 4 mM Cl^- have been fit by Eq. 2, suggesting a $z\delta$ of −1.17 ± 0.11. In both A and C, the dotted line represents the 0 current level. Mean of data from three to six patches in B and D.

ATP had no effect on E1371Q and only a very small inhibitory effect on K95S/S1141K/E1371Q (Fig. 6 B).

Interestingly, the inhibition of S1141K/E1371Q by intracellular ATP was very much weaker when using a high extracellular Cl^- concentration (154 mM; Fig. 6 C) during voltage steps of the same duration. Slow, time-dependent inhibition is apparent only at the most negative voltages studied under these conditions. The concentration dependence of block at −100 mV is shown in Fig. 6 D, and fitting by Eq. 3 suggests a K_d of 36.3 mM, although because this is much greater than the highest concentration of ATP actually used, it is unlikely to be a reliable value.

Voltage dependence of ATP block studied in this way is shown in Fig. 6 E. With low extracellular Cl^-, K_d increased rapidly with depolarization. Fitting these data with Eq. 2 suggests a zδ of −1.17, although the meaning of this value is complicated by uncertainty as to the valence of ATP species actually blocking the channel (see Discussion). Because block under high extracellular Cl^- conditions could only be quantified at the most hyperpolarized voltages studied, voltage dependence of block under these conditions could not be examined.

The apparent voltage-dependent block of S1141K by ATP, and likely also by PPi (Fig. 5), complicated studies of the interaction of this mutant with open-channel blockers like those studied in Fig. 1 and Fig. S1. Nevertheless, we were able to study NPPB block of S1141K under conditions where ATP block was weak (by using symmetrical Cl^- conditions) and in the absence of PPi. Under these conditions, a low concentration of NPPB (10 µM) had significantly more potent blocking effects on S1141K than on wild type (Fig. S5).

The novel apparent inhibitory effects of ATP and PPi seen in S1141K but not in wild type suggest that this mutant might be particularly susceptible to block by polyvalent anions. Few small polyvalent anions have been described as open-channel blockers in CFTR; however, one such ion is the divalent $Pt(NO_2)_4^{2-}$ (Gong and Linsdell, 2003; Zhou et al., 2007). Under ATP-free conditions, block by intracellular $Pt(NO_2)_4^{2-}$ was dramatically more potent in E1371Q/S1141K compared with E1371Q alone, leading to a 38-fold decrease in mean $K_d(0)$ (Fig. S6). This result is consistent with the S1141K mutation preferentially increasing the strength of interactions between polyvalent anions and the pore.

Adding an extra positive charge to the inner vestibule of the pore decreases channel current in intact cells

Because S1141K shows increased sensitivity to inhibition by intracellular anions such as ATP (Fig. 6), PPi (Fig. 5), NPPB (Fig. S5), and $Pt(NO_2)_4^{2-}$ (Fig. S6), we wondered if this sensitivity would result in inhibition of channel currents in intact cells. CFTR channel currents are known to be subject to voltage-dependent inhibition by unknown anions present in the cytosol (Tabcharani et al., 1991; Haws et al., 1992; Fischer and Machen, 1996; Linsdell and Hanrahan, 1996b; Zhou et al., 2001). We took advantage of constitutive activity of E1371Q in BHK cells (see above) to monitor channel block in intact cells. CFTR activity was monitored using a voltage step protocol, both during on-cell recording and after patch excision into the inside-out configuration in the absence of ATP and PKA (Fig. 7). The extracellular (pipette) solution contained either 154 or 4 mM Cl^-. In all cases, the identity of CFTR currents was confirmed by the addition of 10 µM $CFTR_{inh}$-172 to the intracellular solution at the end of the experiment (see Materials and methods).

With high Cl^- concentration pipette solution, E1371Q showed outward rectification of the macroscopic I-V relationship during cell-attached recording (Fig. 7, A and B). This rectification was removed when the membrane patch was excised into the inside-out configuration (Fig. 7, A and B), presumably due to relief of voltage-dependent channel block caused by cytoplasmic anions. Outward rectification in cell-attached patches under these conditions was even more pronounced in S1141K/E1371Q, and again this rectification was relieved by excision of the membrane patch, resulting in a linear I-V relationship in inside-out patches. Using pipette solutions containing a low Cl^- concentration (Fig. 7, A and B), current amplitudes were small during cell-attached recording and increased dramatically on excision to the inside-out configuration, again consistent with currents being inhibited by cytoplasmic factors during cell-attached recordings.

The apparent inhibition of current in cell-attached patches, attributed to block by cytosolic constituents, was quantified from the ratio of macroscopic current amplitudes before and after patch excision (Fig. 7, C and D). Such analysis revealed that current inhibition in cell-attached patches was significantly stronger in S1141K/E1371Q than in E1371Q at hyperpolarized voltages, both at high extracellular Cl^- concentrations (Fig. 7 C) and at low Cl^- concentrations (Fig. 7 D). We interpret this difference as being the result of increased susceptibility to voltage-dependent block by cytoplasmic anions caused by the introduction of a second positive charge in this region of the inner vestibule of the pore.

DISCUSSION

An important positive charge can be moved around the inner vestibule

The positive charge at K95 in TM1 plays a crucial role in Cl^- permeation through the CFTR pore, most likely due to the electrostatic attraction of cytoplasmic anions into the pore (Linsdell, 2005). However, the effects of complementary mutations at K95 and at S1141 in TM12 suggest that the important functional role of this positive

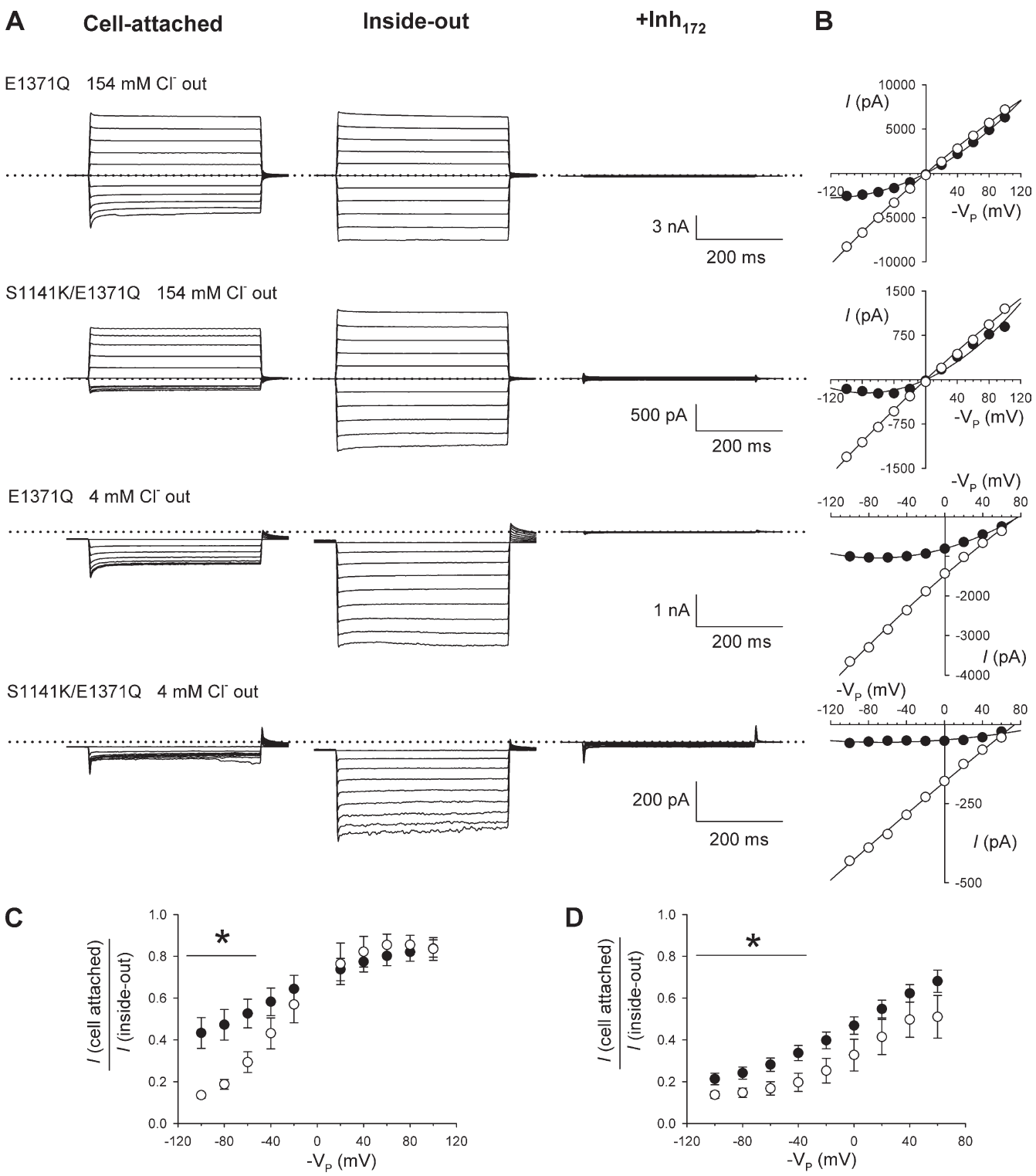

Figure 7. Enhanced voltage-dependent inhibition in cell-attached patches in S1141K-CFTR. (A) Example macroscopic currents carried by E1371Q and S1141K/E1371Q-CFTR in cell-attached patches (left panels) after excision into the inside-out patch configuration (middle panels) and after the addition of 10 μM $CFTR_{inh}$-172 to the intracellular solution (right panels). Currents were recorded with either a high (154-mM) or low (4-mM) Cl^- concentration in the extracellular solution as noted. No PKA, ATP, or PPi was added to the bath solution during these experiments. With 154 mM Cl^- outside, currents were recorded during voltage steps from a holding potential of 0 mV to between −100 and +100 mV, whereas with 4 mM Cl^-, voltage steps were from a holding potential of +60 mV to between −100 and +60 mV. In each case, the 0 current level is indicated by a dotted line. (B) Corresponding I-V relationships during cell-attached (●) and inside-out patch recording (○) after the subtraction of leak currents recorded after the addition of $CFTR_{inh}$-172. (C and D) Quantification of the voltage-dependent inhibition of currents during cell-attached recording by plotting the macroscopic

charge can be retained even after it has been moved to another TM. The similarity of wild type and K95S/S1141K in terms of single-channel conductance (Fig. 2) and interactions with open-channel blockers (Fig. 1 and Fig. S1) suggests that these two residues are almost completely interchangeable in functional terms. Furthermore, we suggest that irreversible inhibition of channel function in the K95C/S1141C double mutant by the oxidizing agent CuPhe (Fig. 3) most likely reflects formation of a disulfide bridge between these two pore-lining cysteine side chains (Fig. 4). The inhibition of channel function by CuPhe may reflect a decrease in unitary conductance or open probability in cross-linked channels, although because the inhibitory effect of CuPhe appears voltage dependent (Fig. 3), we favor the former explanation. Regardless of their exact functional consequence, for such disulfide bonds to form, it is generally believed the β carbon distance must be in the range of ∼5–8 Å (Careaga and Falke, 1992). Thus, we suggest that TM1 and TM12 are located close together in the inner vestibule of the pore, such that the K95S/S1141K double mutant involves transplantation of fixed positive charge over a short distance. The apparent functional interchangeability of K95 and S1141 suggested by our results implies that it is the presence of a positive charge in this region of the inner vestibule of the pore—rather than its exact location within TM1—that is necessary for the normal functional properties of the CFTR pore.

It has previously been suggested that S1141 may play a similar role as S341 in TM6 (McDonough et al., 1994). However, it did not appear that the positive charge of K95 could be transplanted to S341 without large changes in channel functional properties. Thus, both S341K and K95S/S341K were associated with very low single-channel conductance (Fig. S2). This is consistent with previous work, for example with S341A (McDonough et al., 1994), showing that mutations at this position are associated with dramatic loss of Cl^- conductance. However, a positive charge at position 341 could support interactions with open-channel blockers (Fig. 1 and Fig. S1). This might indicate that interactions with blockers are less sensitive to the precise location of a positive charge in the inner vestibule than is normal Cl^- conductance. This would not be surprising in evolutionary terms because maximization of Cl^- conductance is the physiologically meaningful role of the positive charge associated with K95 in this part of the inner vestibule of the pore, with interaction with channel blockers a somewhat detrimental "side effect" of this charge in the permeation pathway.

CFTR open-channel blockers have previously been suggested to interact with residues in TM1 (Linsdell, 2005), TM6 (McDonough et al., 1994; Zhang et al., 2000; Gupta and Linsdell, 2002), and TM12 (McDonough et al., 1994; Zhang et al., 2000; Gupta and Linsdell, 2002). The ability of a positive charge located in TM1 (K95), TM6 (S341K), or TM12 (S1141K) to support blocker interactions is consistent with each of these TMs influencing the movement of blocking anions in the pore. Because these compounds are thought to act by occluding the channel pore to prevent Cl^- permeation, we assume that the effect of mutations is to alter the access of blockers to their binding site (changing blocker on-rate) or the stability of blocker interactions with their binding site (changing blocker off-rate), or both. A change in blocker on-rate could reflect an electrostatic effect of the positive charge on entry of negatively charged blockers into the inner vestibule of the pore. On the other hand, a change in blocker off-rate could result from a positive charge being an integral part of the blocker-binding site.

Our experiments with intracellular application of MTS reagents (Fig. 4) suggest that TM1, TM6, and TM12 are all exposed within the inner vestibule of the pore, where they could, in theory, interact directly with open-channel blockers. This overall arrangement of TMs is consistent with extant atomic models of the CFTR pore that are based on homology modeling of the bacterial ATP-binding cassette protein Sav1866 (Mornon et al., 2008; Serohijos et al., 2008) (Fig. S7). However, direct experimental evidence concerning the three-dimensional architecture of the pore is only now beginning to emerge (Alexander et al., 2009). Our cross-linking experiments showing the proximity of K95 in TM1 and S1141 in TM12 therefore represent important new information in judging the accuracy of these structural models (Fig. S7). Interestingly, the homology model presented by Mornon et al. (2008) provides a possible structural explanation of our results concerning the roles of K95, S341, and S1141. In this model (Fig. S7, A and B), K95 and S1141 are close together (closest atomic distance, 9.6 Å) in the inner vestibule of the pore, where they could play interchangeable roles in interacting within intracellular Cl^- and blocking ions. In contrast, this model shows S341 located more deeply into the pore from its cytoplasmic mouth, consistent with mutations here (potentially close to the narrow

current amplitude in cell-attached patches as a fraction of current in the same patch after excision into the inside-out patch configuration for both E1371Q (●) and S1141K/E1371Q (○), with 154 mM Cl^- (C) or 4 mM Cl^- (D) in the extracellular solution. Mean of data from four to six patches. Asterisk indicates the voltage range over which there was a significant difference between these two channel variants ($P < 0.05$).

pore region) having a more disruptive effect on unitary Cl^- conductance.

Interestingly, not only apparent blocker affinity, but also voltage dependence was affected by removal of the crucial positive charge at K95 (Fig. 1 and Fig. S1). The apparent valence of both TLCS and lonidamine was significantly reduced in K95S, although the apparent valence for NPPB was not significantly altered by this mutation. The meaning of the voltage dependence of the residual block observed in K95S is not clear, and because block is so weak in this mutant, we are reluctant to attach any physical meaning to the apparent valence. Interestingly, in all cases, blocker apparent valence was not significantly different between wild type and double mutants showing restored blocker binding (K95S/S341K, K95S/S1141K), suggesting that blocker movement in the TM electric field was well conserved in these mutants.

Impact of the number of positive charges in the inner vestibule of the pore

Our group has surveyed the effects of neutralization of all positive charges in the TMs of CFTR (Linsdell, 2005; St. Aubin et al., 2007; Zhou et al., 2008), with the exception of R347 in TM6, which is known to form a salt bridge with a negatively charged amino acid side chain (D924) in TM8 (Cotten and Welsh, 1999). Lysine K95 appears to play a unique role relatively deep within the inner vestibule of the pore, with other charges (R303 and perhaps R352) being located more superficially at the cytoplasmic mouth of the pore (see Introduction). The apparent functional interchangeability and physical proximity of K95 and S1141 allowed us to explore the consequences of increasing the number of positive charges in this region of the inner vestibule of the pore apparently available to interact with cytoplasmic anions from one (as we assume to exist in wild type) to two (in the S1141K mutant).

Although increasing the number of positive charges in a localized region of the inner vestibule of the pore (according to this model) from 0 (in K95S) to one (wild type and K95S/S1141K) was associated with a dramatic increase in Cl^- conductance (Fig. 2), increasing further to two positive charges (S1141K) actually led to a slight decrease in conductance (Fig. 2). This suggests that an optimal electrostatic attraction on cytoplasmic Cl^- ions can be achieved with only one positive charge at this location in the pore, and that factors other than electrostatic attraction may set the upper limit on conductance in wild-type CFTR. For example, it has been shown that mutations at T338 in the pore narrow region can increase Cl^- conductance above wild-type values, perhaps by widening the pore in this region and decreasing the rate-limiting resistance to Cl^- flow (Linsdell et al., 1998; Fatehi et al., 2007).

Although S1141K was no better than wild type in terms of Cl^- conductance, it did show an increased sensitivity to block by intracellular anions. This first became apparent to us as a novel sensitivity to block by intracellular ATP molecules (Fig. 6), although it appears that S1141K also increases sensitivity to PPi (Fig. 5), NPPB (Fig. S5), and $Pt(NO_2)_4^{2-}$ (Fig. S6). Block by intracellular ATP appears as a voltage- and extracellular $[Cl^-]$–dependent phenomenon (Fig. 6), suggesting that negatively charged ATP molecules are attracted into the pore of S1141K-CFTR by the increased number of fixed positive charges in the inner vestibule of this mutant. We note that this pore-blocking inhibitory effect is mechanistically distinct from any "allosteric" inhibitory action that may be exhibited by substances that interact with the nucleotide-binding domains in CFTR (see Li and Sheppard, 2009).

Another complication relating to ATP block is that we made no attempt to separate the effects of different charged species of ATP. Under our experimental conditions, $MgATP^{2-}$ is expected to be the dominant species at low total ATP concentrations; however, its relative contribution to total ATP decreases at higher concentrations with concomitant increases in the relative contribution of $NaATP^{3-}$ and ATP^{4-} (as described in Table I). Although our analyses have treated ATP as a single species, it is likely that different charged species will have different blocking affinities and voltage dependencies. Nevertheless, we believe that the ability of physiologically relevant ATP molecules to enter into and block the channel pore (and their apparent lack of effect in wild type) is of interest, in particular given previous controversies relating to the ability of ATP to be transported by CFTR (for review see Schwiebert, 1999).

Given our uncertainty concerning which species of ATP are responsible for block of S1141K, it is difficult to draw conclusions on the relative effect of an additional fixed positive charge at this position on interactions with monovalent versus polyvalent anions. It seems likely that block by both ATP and PPi represents an inhibitory effect of polyvalent anions that is too weak to be noticeable in wild-type channels. Consistent with this, the apparent affinity of block by small, divalent $Pt(NO_2)_4^{2-}$ anions was increased ~38-fold in S1141K/E1371Q compared with E1371Q (Fig. S6). In contrast, S1141K had a more modest effect on block by the larger, monovalent organic anion NPPB (Fig. S5), with the apparent K_d for this blocker being increased less than fourfold under different experimental conditions. Based on this highly limited survey of blocking anions, it seems reasonable to suggest that the additional positive charge present in the pore of S1141K channels favors interactions with polyvalent anions. An analogous situation has been described in K^+ channel pores, where fixed negative charges in the channel protein preferentially attract polyvalent cationic blockers into the pore compared with monovalent K^+ ions, leading to channel block and current rectification (Zhang et al., 2006).

Although block by ATP was apparent in our initial experiments in inside-out patches, we were most interested to observe CFTR current inhibition under the more physiological conditions provided by intact cells (Fig. 7). It has long been suggested that CFTR channel currents in intact cells are inhibited at hyperpolarized voltages due to open-channel block by unknown cytosolic anions (Tabcharani et al., 1991; Haws et al., 1992; Fischer and Machen, 1996; Linsdell and Hanrahan, 1996b; Zhou et al., 2001). As shown in Fig. 7, this inhibition is pronounced in BHK cells, leading to an ~60% block of wild-type (actually E1371Q) currents in intact cells at −100 mV with high extracellular Cl^-. The apparent degree of block increased to almost 80% at low extracellular Cl^-, suggesting that endogenous cytoplasmic-blocking anions, like well-characterized CFTR open-channel blockers (Linsdell and Hanrahan, 1996b; Sheppard and Robinson, 1997; Linsdell and Hanrahan, 1999), are susceptible to "knock off" by extracellular Cl^- ions (Zhou et al., 2001). Although block appears strong in wild type (E1371Q), it is still significantly strengthened in S1141K (Fig. 7), suggesting that the number of fixed positive charges in the inner vestibule of the pore controls interactions with endogenous cytoplasmic-blocking molecules, and therefore (in intact cells) overall channel function in terms of the rate of anion efflux.

Implications for the mechanism of Cl^- permeation

One positive charge around the location normally occupied by K95 in the inner vestibule of the pore is essential for CFTR Cl^- channel function, as indicated by the fact that removing this charge leads to a drastic decrease in Cl^- conductance (Ge et al., 2004) (Fig. 2). However, increasing the number of functionally analogous positive charges in this region of the pore from one to two has an overall detrimental effect on channel function, as it fails to increase Cl^- conductance but at the same time increases susceptibility to block by cytoplasmic anions. This may be because the presence of an additional positive charge favors attraction of polyvalent anions into the pore, whereas the normal substrates of CFTR-mediated transport (Cl^- and HCO_3^-) are monovalent anions. An overall decrease in channel function in intact cells is demonstrated in on-cell current recordings (Fig. 7), which show decreased Cl^- currents (relative to unblocked currents after patch excision to the inside-out configuration) at hyperpolarized voltages in S1141K/E1371Q relative to E1371Q alone. In other channel types, "rings" of fixed charge surrounding the permeation pathway may act to maximize channel conductance (Imoto et al., 1988; Chiamvimonvat et al., 1996; Brelidze et al., 2003; Haug et al., 2004). In contrast, at the level of K95 in the inner vestibule of the CFTR pore, optimal channel function appears to be achieved with just a single fixed positive charge.

We thank Dr. David Gadsby for providing the cys-less CFTR cDNA.

This work was supported by the Canadian Institutes of Health Research.

Christopher Miller served as editor.

Submitted: 18 September 2009
Accepted: 19 January 2010

REFERENCES

Alexander, C., A. Ivetac, X. Liu, Y. Norimatsu, J.R. Serrano, A. Landstrom, M. Sansom, and D.C. Dawson. 2009. Cystic fibrosis transmembrane conductance regulator: using differential reactivity toward channel-permeant and channel-impermeant thiol-reactive probes to test a molecular model for the pore. *Biochemistry.* 48:10078–10088. doi:10.1021/bi901314c

Brelidze, T.I., X. Niu, and K.L. Magleby. 2003. A ring of eight conserved negatively charged amino acids doubles the conductance of BK channels and prevents inward rectification. *Proc. Natl. Acad. Sci. USA.* 100:9017–9022. doi:10.1073/pnas.1532257100

Brooks, S.P.J., and K.B. Storey. 1992. Bound and determined: a computer program for making buffers of defined ion concentrations. *Anal. Biochem.* 201:119–126. doi:10.1016/0003-2697(92)90183-8

Careaga, C.L., and J.J. Falke. 1992. Structure and dynamics of *Escherichia coli* chemosensory receptors. Engineered sulfhydryl studies. *Biophys. J.* 62:209–219. doi:10.1016/S0006-3495(92)81806-4

Chiamvimonvat, N., M.T. Pérez-García, G.F. Tomaselli, and E. Marban. 1996. Control of ion flux and selectivity by negatively charged residues in the outer mouth of rat sodium channels. *J. Physiol.* 491:51–59.

Cotten, J.F., and M.J. Welsh. 1999. Cystic fibrosis-associated mutations at arginine 347 alter the pore architecture of CFTR. Evidence for disruption of a salt bridge. *J. Biol. Chem.* 274:5429–5435. doi:10.1074/jbc.274.9.5429

Cui, G., Z.-R. Zhang, A.R.W. O'Brien, B. Song, and N.A. McCarty. 2008. Mutations at arginine 352 alter the pore architecture of CFTR. *J. Membr. Biol.* 222:91–106. doi:10.1007/s00232-008-9105-9

Fatehi, M., and P. Linsdell. 2009. Novel residues lining the CFTR chloride channel pore identified by functional modification of introduced cysteines. *J. Membr. Biol.* 228:151–164. doi:10.1007/s00232-009-9167-3

Fatehi, M., C.N. St. Aubin, and P. Linsdell. 2007. On the origin of asymmetric interactions between permeant anions and the cystic fibrosis transmembrane conductance regulator chloride channel pore. *Biophys. J.* 92:1241–1253. doi:10.1529/biophysj.106.095349

Fischer, H., and T.E. Machen. 1996. The tyrosine kinase $p60^{c\text{-}src}$ regulates the fast gate of the cystic fibrosis transmembrane conductance regulator chloride channel. *Biophys. J.* 71:3073–3082. doi:10.1016/S0006-3495(96)79501-2

Gadsby, D.C., P. Vergani, and L. Csanády. 2006. The ABC protein turned chloride channel whose failure causes cystic fibrosis. *Nature.* 440:477–483. doi:10.1038/nature04712

Ge, N., C.N. Muise, X. Gong, and P. Linsdell. 2004. Direct comparison of the functional roles played by different transmembrane regions in the cystic fibrosis transmembrane conductance regulator chloride channel pore. *J. Biol. Chem.* 279:55283–55289. doi:10.1074/jbc.M411935200

Gong, X., and P. Linsdell. 2003. Mutation-induced blocker permeability and multiion block of the CFTR chloride channel pore. *J. Gen. Physiol.* 122:673–687. doi:10.1085/jgp.200308889

Gong, X., S.M. Burbridge, E.A. Cowley, and P. Linsdell. 2002a. Molecular determinants of $Au(CN)_2^-$ binding and permeability within the cystic fibrosis transmembrane conductance regulator Cl^- channel pore. *J. Physiol.* 540:39–47. doi:10.1113/jphysiol.2001.013235

Gong, X., S.M. Burbridge, A.C. Lewis, P.Y.D. Wong, and P. Linsdell. 2002b. Mechanism of lonidamine inhibition of the CFTR chloride channel. *Br. J. Pharmacol.* 137:928–936. doi:10.1038/sj.bjp.0704932

Gupta, J., and P. Linsdell. 2002. Point mutations in the pore region directly or indirectly affect glibenclamide block of the CFTR chloride channel. *Pflugers Arch.* 443:739–747. doi:10.1007/s00424-001-0762-0

Haug, T., D. Sigg, S. Ciani, L. Toro, E. Stefani, and R. Olcese. 2004. Regulation of K^+ flow by a ring of negative charges in the outer pore of BK_{Ca} channels. Part I: aspartate 292 modulates K^+ conduction by external surface charge effect. *J. Gen. Physiol.* 124:173–184. doi:10.1085/jgp.200308949

Haws, C., M.E. Krouse, Y. Xia, D.C. Gruenert, and J.J. Wine. 1992. CFTR channels in immortalized human airway cells. *Am. J. Physiol.* 263:L692–L707.

Hwang, T.-C., and D.N. Sheppard. 2009. Gating of the CFTR Cl^- channel by ATP-driven nucleotide-binding domain dimerisation. *J. Physiol.* 587:2151–2161. doi:10.1113/jphysiol.2009.171595

Imoto, K., C. Busch, B. Sakmann, M. Mishina, T. Konno, J. Nakai, H. Bujo, Y. Mori, K. Fukuda, and S. Numa. 1988. Rings of negatively charged amino acids determine the acetylcholine receptor channel conductance. *Nature.* 335:645–648. doi:10.1038/335645a0

Kidd, J.F., I. Kogan, and C.E. Bear. 2004. Molecular basis for the chloride channel activity of cystic fibrosis transmembrane conductance regulator and the consequences of disease-causing mutations. *Curr. Top. Dev. Biol.* 60:215–249. doi:10.1016/S0070-2153(04)60007-X

Li, H., and D.N. Sheppard. 2009. Therapeutic potential of cystic fibrosis transmembrane conductance regulator (CFTR) inhibitors in polycystic kidney disease. *BioDrugs.* 23:203–216. doi:10.2165/11313570-000000000-00000

Li, M.-S., A.F.A. Demsey, J. Qi, and P. Linsdell. 2009. Cysteine-independent inhibition of the CFTR chloride channel by the cysteine-reactive reagent sodium (2-sulphonatoethyl) methanethiosulphonate. *Br. J. Pharmacol.* 157:1065–1071. doi:10.1111/j.1476-5381.2009.00258.x

Linsdell, P. 2005. Location of a common inhibitor binding site in the cytoplasmic vestibule of the cystic fibrosis transmembrane conductance regulator chloride channel pore. *J. Biol. Chem.* 280:8945–8950. doi:10.1074/jbc.M414354200

Linsdell, P. 2006. Mechanism of chloride permeation in the cystic fibrosis transmembrane conductance regulator chloride channel. *Exp. Physiol.* 91:123–129. doi:10.1113/expphysiol.2005.031757

Linsdell, P., and X. Gong. 2002. Multiple inhibitory effects of $Au(CN)_2^-$ ions on cystic fibrosis transmembrane conductance regulator Cl^- channel currents. *J. Physiol.* 540:29–38. doi:10.1113/jphysiol.2001.013234

Linsdell, P., and J.W. Hanrahan. 1996a. Disulphonic stilbene block of cystic fibrosis transmembrane conductance regulator Cl^- channels expressed in a mammalian cell line and its regulation by a critical pore residue. *J. Physiol.* 496:687–693.

Linsdell, P., and J.W. Hanrahan. 1996b. Flickery block of single CFTR chloride channels by intracellular anions and osmolytes. *Am. J. Physiol.* 271:C628–C634.

Linsdell, P., and J.W. Hanrahan. 1998. Adenosine triphosphate–dependent asymmetry of anion permeation in the cystic fibrosis transmembrane conductance regulator chloride channel. *J. Gen. Physiol.* 111:601–614. doi:10.1085/jgp.111.4.601

Linsdell, P., and J.W. Hanrahan. 1999. Substrates of multidrug resistance-associated proteins block the cystic fibrosis transmembrane conductance regulator chloride channel. *Br. J. Pharmacol.* 126:1471–1477. doi:10.1038/sj.bjp.0702458

Linsdell, P., S.-X. Zheng, and J.W. Hanrahan. 1998. Non-pore lining amino acid side chains influence anion selectivity of the human CFTR Cl^- channel expressed in mammalian cell lines. *J. Physiol.* 512:1–16. doi:10.1111/j.1469-7793.1998.001bf.x

Loo, T.W., M.C. Bartlett, and D.M. Clarke. 2008. Processing mutations disrupt interactions between the nucleotide binding and transmembrane domains of P-glycoprotein and the cystic fibrosis transmembrane conductance regulator (CFTR). *J. Biol. Chem.* 283:28190–28197. doi:10.1074/jbc.M805834200

Ma, T., J.R. Thiagarajah, H. Yang, N.D. Sonawane, C. Folli, L.J.V. Galietta, and A.S. Verkman. 2002. Thiazolidinone CFTR inhibitor identified by high-throughput screening blocks cholera toxin-induced intestinal fluid secretion. *J. Clin. Invest.* 110:1651–1658.

McCarty, N.A. 2000. Permeation through the CFTR chloride channel. *J. Exp. Biol.* 203:1947–1962.

McDonough, S., N. Davidson, H.A. Lester, and N.A. McCarty. 1994. Novel pore-lining residues in CFTR that govern permeation and open-channel block. *Neuron.* 13:623–634. doi:10.1016/0896-6273(94)90030-2

Mense, M., P. Vergani, D.M. White, G. Altberg, A.C. Nairn, and D.C. Gadsby. 2006. In vivo phosphorylation of CFTR promotes formation of a nucleotide-binding domain heterodimer. *EMBO J.* 25:4728–4739. doi:10.1038/sj.emboj.7601373

Mio, K., T. Ogura, M. Mio, H. Shimizu, T.-C. Hwang, C. Sato, and Y. Sohma. 2008. Three-dimensional reconstruction of human cystic fibrosis transmembrane conductance regulator chloride channel revealed an ellipsoidal structure with orifices beneath the putative transmembrane domain. *J. Biol. Chem.* 283:30300–30310. doi:10.1074/jbc.M803185200

Mornon, J.-P., P. Lehn, and I. Callebaut. 2008. Atomic model of human cystic fibrosis transmembrane conductance regulator: membrane-spanning domains and coupling interfaces. *Cell. Mol. Life Sci.* 65:2594–2612. doi:10.1007/s00018-008-8249-1

Muallem, D., and P. Vergani. 2009. Review. ATP hydrolysis-driven gating in cystic fibrosis transmembrane conductance regulator. *Philos. Trans. R. Soc. Lond. B Biol. Sci.* 364:247–255. doi:10.1098/rstb.2008.0191

Rosenberg, M.F., A.B. Kamis, L.A. Aleksandrov, R.C. Ford, and J.R. Riordan. 2004. Purification and crystallization of the cystic fibrosis transmembrane conductance regulator (CFTR). *J. Biol. Chem.* 279:39051–39057. doi:10.1074/jbc.M407434200

Schwiebert, E.M. 1999. ABC transporter-facilitated ATP conductive transport. *Am. J. Physiol.* 276:C1–C8.

Serohijos, A.W.R., T. Hegedüs, A.A. Aleksandrov, L. He, L. Cui, N.V. Dokholyan, and J.R. Riordan. 2008. Phenylalanine-508 mediates a cytoplasmic-membrane domain contact in the CFTR 3D structure crucial to assembly and channel function. *Proc. Natl. Acad. Sci. USA.* 105:3256–3261. doi:10.1073/pnas.0800254105

Sheppard, D.N., and K.A. Robinson. 1997. Mechanism of glibenclamide inhibition of cystic fibrosis transmembrane conductance regulator Cl^- channels expressed in a murine cell line. *J. Physiol.* 503:333–346. doi:10.1111/j.1469-7793.1997.333bh.x

Smith, S.S., X. Liu, Z.-R. Zhang, F. Sun, T.E. Kriewall, N.A. McCarty, and D.C. Dawson. 2001. CFTR: covalent and noncovalent modification suggests a role for fixed charges in anion conduction. *J. Gen. Physiol.* 118:407–431. doi:10.1085/jgp.118.4.407

St. Aubin, C.N., and P. Linsdell. 2006. Positive charges at the intracellular mouth of the pore regulate anion conduction in the CFTR chloride channel. *J. Gen. Physiol.* 128:535–545. doi:10.1085/jgp.200609516

St Aubin, C.N., J.-J. Zhou, and P. Linsdell. 2007. Identification of a second blocker binding site at the cytoplasmic mouth of the cystic fibrosis transmembrane conductance regulator chloride channel pore. *Mol. Pharmacol.* 71:1360–1368. doi:10.1124/mol.106.031732

Stratford, F.L.L., M. Ramjeesingh, J.C. Cheung, L.-J. Huan, and C.E. Bear. 2007. The Walker B motif of the second nucleotide-binding domain (NBD2) of CFTR plays a key role in ATPase activity by the NBD1-NBD2 heterodimer. *Biochem. J.* 401:581–586. doi:10.1042/BJ20060968

Tabcharani, J.A., X.-B. Chang, J.R. Riordan, and J.W. Hanrahan. 1991. Phosphorylation-regulated Cl^- channel in CHO cells stably expressing the cystic fibrosis gene. *Nature.* 352:628–631. doi:10.1038/352628a0

Vergani, P., A.C. Nairn, and D.C. Gadsby. 2003. On the mechanism of MgATP-dependent gating of CFTR Cl^- channels. *J. Gen. Physiol.* 121:17–36. doi:10.1085/jgp.20028673

Woodhull, A.M. 1973. Ionic blockage of sodium channels in nerve. *J. Gen. Physiol.* 61:687–708. doi:10.1085/jgp.61.6.687

Zhang, Y., X. Niu, T.I. Brelidze, and K.L. Magleby. 2006. Ring of negative charge in BK channels facilitates block by intracellular Mg^{2+} and polyamines through electrostatics. *J. Gen. Physiol.* 128:185–202. doi:10.1085/jgp.200609493

Zhang, Z.-R., S. Zeltwanger, and N.A. McCarty. 2000. Direct comparison of NPPB and DPC as probes of CFTR expressed in *Xenopus* oocytes. *J. Membr. Biol.* 175:35–52. doi:10.1007/s002320001053

Zhou, J.-J., M. Fatehi, and P. Linsdell. 2007. Direct and indirect effects of mutations at the outer mouth of the cystic fibrosis transmembrane conductance regulator chloride channel pore. *J. Membr. Biol.* 216:129–142. doi:10.1007/s00232-007-9056-6

Zhou, J.-J., M. Fatehi, and P. Linsdell. 2008. Identification of positive charges situated at the outer mouth of the CFTR chloride channel pore. *Pflugers Arch.* 457:351–360. doi:10.1007/s00424-008-0521-6

Zhou, Z., S. Hu, and T.-C. Hwang. 2001. Voltage-dependent flickery block of an open cystic fibrosis transmembrane conductance regulator (CFTR) channel pore. *J. Physiol.* 532:435–448. doi:10.1111/j.1469-7793.2001.0435f.x